

High detection efficiency micro-structured solid-state neutron detector with extremely low leakage current fabricated with continuous p-n junction

Kuan-Chih Huang,¹ Rajendra Dahal,^{1,2} James J.-Q. Lu,¹ Yaron Danon,² and Ishwara B. Bhat^{1,a)}

¹Department of Electrical, Computer, and Systems Engineering, Rensselaer Polytechnic Institute, Troy, New York 12180-3522, USA

²Department of Mechanical, Aerospace, and Nuclear Engineering, Rensselaer Polytechnic Institute, Troy, New York 12180-3522, USA

(Received 12 February 2013; accepted 3 April 2013; published online 16 April 2013)

We report the continuous p-n junction formation in honeycomb structured Si diode by *in situ* boron deposition and diffusion process using low pressure chemical vapor deposition for solid-state thermal neutron detection applications. Optimized diffusion temperature of 800 °C was obtained by current density-voltage characteristics for fabricated p⁺-n diodes. A very low leakage current density of $\sim 2 \times 10^{-8}$ A/cm² at -1 V was measured for enriched boron filled honeycomb structured neutron detector with a continuous p⁺-n junction. The neutron detection efficiency for a Maxwellian spectrum incident on the face of the detector was measured under zero bias voltage to be $\sim 26\%$. These results are very encouraging for fabrication of large area solid-state neutron detector that could be a viable alternative to ³He tube based technology. © 2013 AIP Publishing LLC
[\[http://dx.doi.org/10.1063/1.4802204\]](http://dx.doi.org/10.1063/1.4802204)

Since neutrons are a very specific indicator of fissile materials, solid-state neutron detectors possessing high neutron detection efficiency, large detection area, and low gamma sensitivity are needed for homeland security as well as civilian applications. Solid-state neutron detectors are better suited in many field applications than the existing gas filled detectors having plenty of drawbacks, such as bulkiness, high bias voltage requirement (1000–2000 V), and high cost due to the limited supply of helium-3.

Solid-state neutron detectors have been demonstrated by coating a thin layer of neutron converter material having large thermal neutron absorption cross-section, such as boron-10 (¹⁰B) or lithium-6 fluoride (⁶LiF), on top of Si or GaAs p-n diodes.^{1–3} Neutron interaction with ¹⁰B results in production of ⁴He and ⁷Li charged particles. As the charged particles escape to the p-n diode, electron-hole pairs (EHPs) are created due to the impact ionization. EHPs created inside the depletion region and within a diffusion length from the depletion region edge are separated by the built-in electric field and then collected as current or voltage pulses by external circuits. In this type of converter-layer-coated planar detector, neutron detection efficiency is limited to only 2%–5% due to the conflicting requirements for large absorption length for neutrons ($\sim 45 \mu\text{m}$ for $\sim 90\%$ interaction of neutrons in ¹⁰B) as well as short escape length for daughter particles (2–3 μm for energetic daughter particles in ¹⁰B).⁴

To overcome this problem, researchers have purposed and demonstrated micro-structured Si p-n diodes filled with ⁶LiF or ¹⁰B in such a way that the converter material is thick enough for neutrons to interact with and at the same time thin enough for daughter particles to escape sideways.^{5,6} Our group has proposed boron filled Si honeycomb structured neutron detector with a continuous p⁺-n junction.⁷ Although the overall neutron detection efficiency of the micro-

structured neutron detector has been increased compared to that of the planar detector, the unpassivated etched Si wall leads to a higher leakage current that increases the device electronic noise, reduces the ability to sense small signals, and ultimately limits the device size.^{5,6,8}

In order to decrease the leakage current, a continuous p⁺-n junction over the entire Si wall was made in our honeycomb structured neutron detectors by using the initial portion of boron filling process followed by boron diffusion process in a low pressure chemical vapor deposition (LPCVD) system.⁹ Making p⁺-n junction continuous in micro-structured p-n diode not only eliminates the surface leakage current from the etched Si wall but also fully depletes the Si wall with the selected doping concentration of p⁺-Si layer and n-Si substrate, which makes the operation of the device without external bias possible. Although the formation of the continuous p⁺-n junction offers a significant improvement and the formation of ultra shallow p⁺-n junction on Si using CVD has been discussed,¹⁰ the effect of boron diffusion process as a part of boron filling process on the detector performance, such as reverse leakage current, depletion width of the vertical Si wall, and bias dependent neutron detection efficiency, has not been studied yet.

In this work, we present the fabrication and characterization of (i) p⁺-n junctions on planar n-Si bulk substrates using the boron deposition and diffusion process with LPCVD at different temperatures (700, 800, and 900 °C), and (ii) enriched boron (99.9% ¹⁰B) filled honeycomb structured thermal neutron detectors with continuous p-n junction over the entire surface using 1 μm thick p⁺-Si and 50 μm thick n-Si epitaxial layers deposited on a n⁺-Si substrate. Boron is selected as a converter material in our present and previous works because it has reasonably high thermal neutron absorption cross-section of ~ 3837 b ($1 \text{ b} = 10^{-24} \text{ cm}^2$) among all kinds of neutron converter materials and also highly compatible with Si processing technology. The current density-voltage (J-V) characteristics of p⁺-n diodes

^{a)}bhati@rpi.edu

fabricated with different diffusion temperatures were studied. Furthermore, reverse leakage current and neutron detection efficiency of a honeycomb structured neutron detector were measured to elucidate the importance of the continuous p^+-n junction.

In order to study the effect of boron diffusion temperature in LPCVD on the J-V characteristics for p^+-n diodes, a 4-in. lightly doped (100) n-Si wafer (bulk Si wafer with resistivity of $\sim 12 \Omega \text{ cm}$) was used as a starting substrate. Ion implantation was performed on the wafer backside to fabricate the $n^+-\text{Si}$ layer (surface doping concentration $\sim 10^{19} \text{ cm}^{-3}$) for ohmic contact. An $\sim 1.5 \mu\text{m}$ thick silicon dioxide (SiO_2) layer was deposited on the front side and then removed from the device area using photolithography and wet buffered oxide etch (BOE). The device size is $2.5 \times 2.5 \text{ mm}^2$ and the devices are isolated with $10 \mu\text{m}$ wide SiO_2 grids. This wafer was diced into four pieces as starting wafers. One starting wafer was used to fabricate Schottky diodes by directly depositing aluminum (Al) with 2% Si on the front side and titanium (Ti)/Al on the backside of the n-Si substrate for metal contacts. On the other three starting wafers, boron was deposited using LPCVD at 510°C for 5 min with a B_2H_6 partial pressure of 0.065 Torr and a $\text{B}_2\text{H}_6/\text{H}_2$ flow rate of 70 standard cubic centimeters per minute (SCCM), followed by boron diffusion in succession in the same reactor for 10 min at 700, 800, and 900°C , respectively, to form $p^+-\text{Si}$ layers. Boron film was removed by wet etching technique (one part of hydrogen peroxide in five part of ethanol by volume at 50°C). Finally, an $\sim 1.5 \mu\text{m}$ thick Al with 2% Si was sputtered on the front side for p-contact and an $\sim 100 \text{ nm}$ thick Ti followed by an $\sim 900 \text{ nm}$ thick Al were sputtered on the backside for n-contact. To isolate devices, front-side metal was removed from the grid area using photolithography and a standard Al wet etching.

Figure 1(a) shows forward-bias and reverse-bias J-V characteristics for a Schottky diode and three p^+-n diodes with boron diffusion at 700, 800, and 900°C . The inset in Fig. 1(a) shows the schematic for p^+-n diode fabricated using n-Si bulk wafer. Boron diffusion at 800 and 900°C results in lower reverse leakage current density on the order of 10^{-6} A/cm^2 at -1 V . However, diffusion at 700°C results in a higher reverse leakage current density on the order of 10^{-4} A/cm^2 at -1 V , which is close to the reverse leakage current of the Schottky diode. It is possible that both Schottky diode behavior and p^+-n diode behavior are observed since the $p^+-\text{Si}$ layer may be very thin and not fully continuous over the entire surface.

Figure 1(b) shows only the forward-bias I-V characteristics for the Schottky diode and the three p^+-n diodes with the ideality factor labeled in different regions. Series resistance is calculated from the deviation of the I-V curve from linearity at high current level. If all three diffusion processes resulted in $p^+-\text{Si}$ layers, the forward-bias and reverse-bias J-V characteristics should be similar for all three p^+-n diodes since the current is mainly determined by the lightly doped n-Si region. Besides, the series resistance of the p^+-n diodes should be significantly lower than that of the Schottky diode due to conductivity modulation in high forward bias. P^+-n diodes with boron diffusion at 800 and 900°C show a reasonably good diode behavior based on the ideality factor and

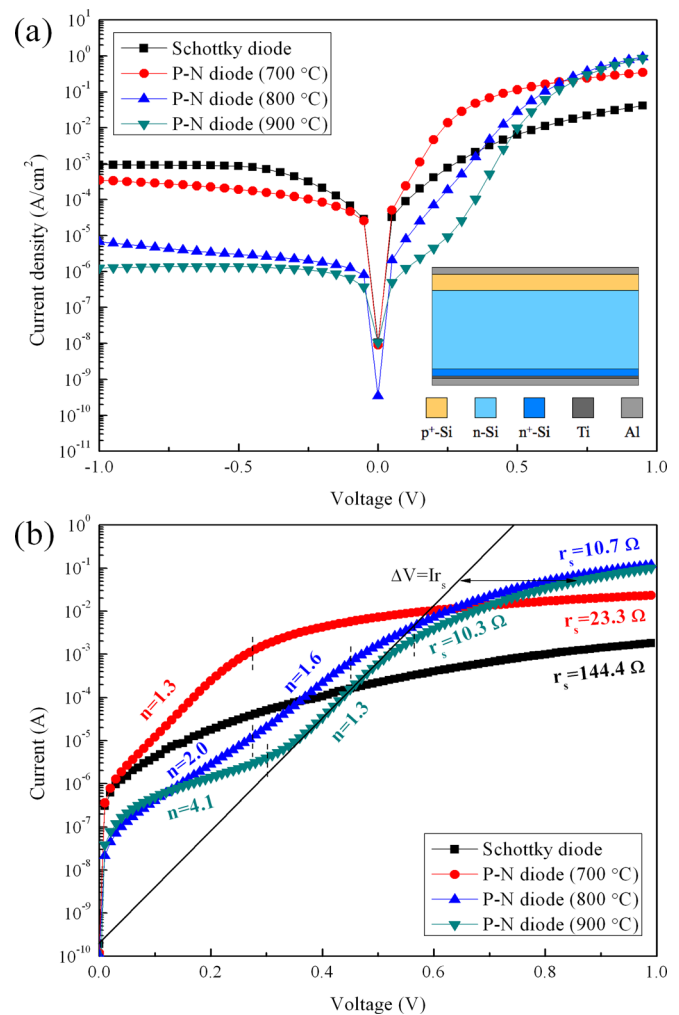


FIG. 1. (a) Forward-bias and reverse-bias J-V characteristics for a Schottky diode and three p^+-n diodes annealed at 700, 800, and 900°C after the boron deposition process. (b) Forward-bias I-V characteristics for a Schottky diode and three p^+-n diodes annealed at 700, 800, and 900°C with the ideality factor labeled in different regions. The inset in Fig. 1(a) shows the schematic for p^+-n diode fabricated using n-Si bulk wafer.

their substantially low reverse leakage current compared to the p^+-n diode with boron diffusion at 700°C . The higher ideality factor of the p^+-n diode with boron diffusion at 900°C at low current level is possibly because of the shunt resistance of the diode. The series resistance of the p^+-n diodes annealed at 800 and 900°C is $\sim 10.3 \Omega$ and $\sim 10.7 \Omega$, which are very close to that of the n-Si bulk wafer ($\sim 9.6 \Omega$) due to low series resistance of the $p^+-\text{Si}$ layers and good metal contacts. As the $p^+-\text{Si}$ layer of the p^+-n diode with boron diffusion at 700°C may be very thin and even not continuous, the series resistance is relatively high ($\sim 23.3 \Omega$). This may be resulted from the contribution of both p^+-n diode and Schottky diode ($\sim 144.4 \Omega$). Based on these results, diffusion temperature of 800°C was chosen to make continuous p^+-n junction in honeycomb structured thermal neutron detector.

In order to verify that the surface leakage current from the etched Si wall in the micro-structured solid-state neutron detector is reduced by the formation of continuous p^+-n junction using *in situ* boron diffusion process, $2.5 \times 2.5 \text{ mm}^2$ planar neutron detector and ^{10}B filled honeycomb structured neutron detector with a continuous p^+-n junction were

fabricated using a Si epitaxial wafer: a 4-in. moderately doped (100) n-Si wafer (resistivity $\sim 0.5 \Omega \text{ cm}$) with an $\sim 50 \mu\text{m}$ thick lightly doped n-Si epitaxial layer ($\sim 50 \Omega \text{ cm}$) and an $\sim 1 \mu\text{m}$ thick heavily doped p-Si epitaxial layer ($\sim 0.01 \Omega \text{ cm}$). Hexagonal holes ($\sim 2.8 \mu\text{m}$ wide by $\sim 42 \mu\text{m}$ deep) were etched into a Si epitaxial wafer using deep reactive ion etching (DRIE) with Bosch process.¹¹ Then, ^{10}B was deposited in these high aspect ratio hexagonal holes using LPCVD. Figure 2(a) shows a cross-sectional SEM image of a conformal boron film deposited in a high aspect ratio hexagonal hole using LPCVD for 30 min. Figures 2(b) and 2(c) are the magnified images of Fig. 2(a) from the top and bottom of the hole, respectively. The thickness of the boron film is $\sim 350 \text{ nm}$ thick outside the hole as well as inside the hole. Since the boron film over the hexagonal holes is very conformal, a very conformal $\text{p}^+\text{-n}$ junction over the entire surface of the microstructure can be formed after boron diffusion at 800°C for 10 min as discussed. After forming the continuous $\text{p}^+\text{-n}$ junction, the hexagonal holes were further filled with ^{10}B in the same LPCVD reactor. The details of honeycomb structured thermal neutron detector are given in our earlier publications.^{9,12} Figure 3 shows the J-V characteristics for the planar neutron detector and the honeycomb structured neutron detector with a continuous $\text{p}^+\text{-n}$ junction. The insets in Fig. 3 show the schematics for planar and the honeycomb structured neutron detectors. The leakage current density for the planar detector is $\sim 2.1 \times 10^{-8} \text{ A/cm}^2$ and that for the honeycomb structured neutron detector with a continuous $\text{p}^+\text{-n}$ junction is $\sim 1.8 \times 10^{-8} \text{ A/cm}^2$ at -1 V , which is more than an order of magnitude lower than our previous result for a similar device structure.¹² This very low reverse leakage current density for our honeycomb structured neutron detector is the lowest among similar micro-structured solid-state neutron detector.^{5,6} Since the reverse leakage current densities for the planar and honeycomb structured detectors are very close, the formation of the continuous $\text{p}^+\text{-n}$ junction in

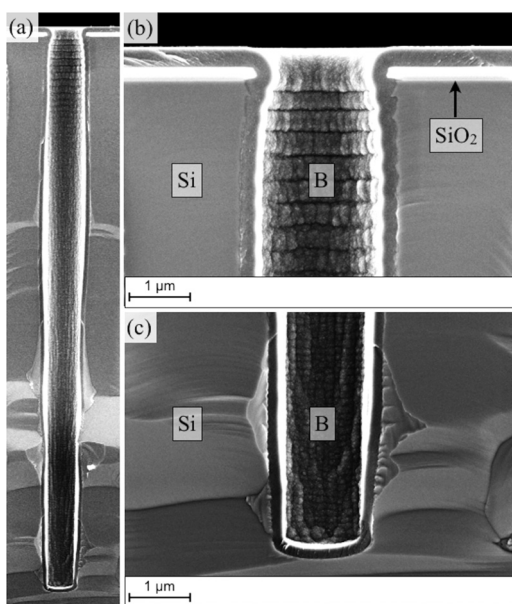


FIG. 2. (a) Cross-sectional SEM image of a conformal boron film deposited in a high aspect ratio hole ($\sim 2.8 \mu\text{m}$ wide by $\sim 42 \mu\text{m}$ deep) fabricated in a Si epitaxial wafer using LPCVD for 30 min. Figures 2(b) and 2(c) are the magnified images of Fig. 2(a) from top and bottom of the hole, respectively.

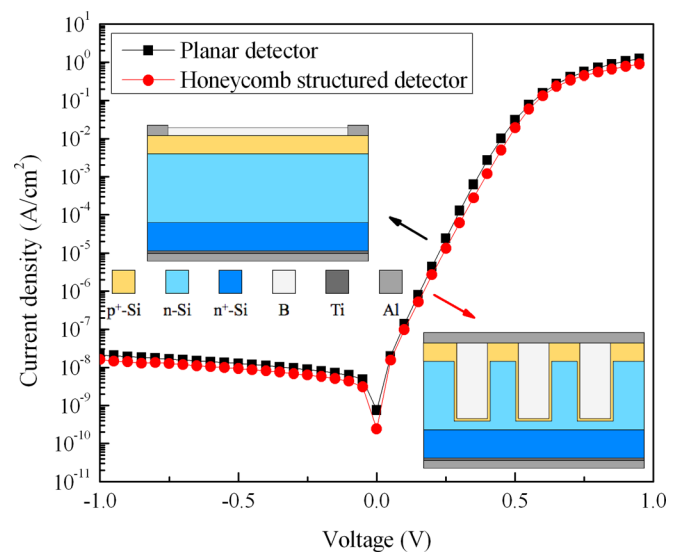


FIG. 3. J-V characteristics for a $2.5 \times 2.5 \text{ mm}^2$ planar neutron detector and a $2.5 \times 2.5 \text{ mm}^2$ honeycomb structured neutron detector with a continuous $\text{p}^+\text{-n}$ junction. The insets show the schematics for planar and the honeycomb structured neutron detectors fabricated using Si epitaxial wafer.

LPCVD as a part of the boron filling process is proven to be effective to reduce the leakage current and thus plays one of the pivotal roles in the fabrication of high-quality micro-structured p-n diodes. Probably because of higher quality epitaxial silicon compared to bulk silicon, the reverse leakage current for the planar and honeycomb structured neutron detectors (fabricated using n-Si epitaxial layer) shown in Fig. 3 is much lower than that for the $\text{p}^+\text{-n}$ diodes (fabricated using n-Si bulk wafer) shown in Fig. 1(a).

Furthermore, a continuous $\text{p}^+\text{-n}$ junction with selected doping concentration of $\text{p}^+\text{-Si}$ layer and n-Si substrate can deplete the Si wall completely. With fully depleted Si wall, the EHPs generated inside the depletion region and one diffusion length away from the edge of the depletion region are separated efficiently by the built-in electric field, which gives rise to a higher neutron detection efficiency under zero bias voltage. In order to verify that the Si wall in the detector is fully depleted, the thermal neutron detection efficiency of the $2.5 \times 2.5 \text{ mm}^2$ ^{10}B filled honeycomb structured neutron detector was measured under different bias voltages. Figure 4 shows measured pulse height distribution for the ^{10}B filled honeycomb structured neutron detector under zero reverse bias voltage with x-axis normalized by assuming the spectrum endpoint is the full charge particle energy deposition ($\sim 2.5 \text{ MeV}$) based on GEANT simulation.¹³ The inset in Fig. 4 shows the neutron detection efficiency as a function of reverse bias voltage. To determine the thermal neutron detection efficiency, an uncollimated neutron beam is created by placing a californium-252 (^{252}Cf) source in a high-density polyethylene moderator housing. Four measurements were conducted for each bias voltage and each measurement was carried out for 3600 s. The detector was placed at a distance of 10 cm, where the average thermal neutron flux was $\sim 798 \text{ neutrons/s/cm}^2$ (black curve).¹² Since not only thermal neutrons but also fast neutrons and gamma rays are emitted by the ^{252}Cf source inside the moderator housing, the moderator housing was covered with a 2 mm thick Cd shield to

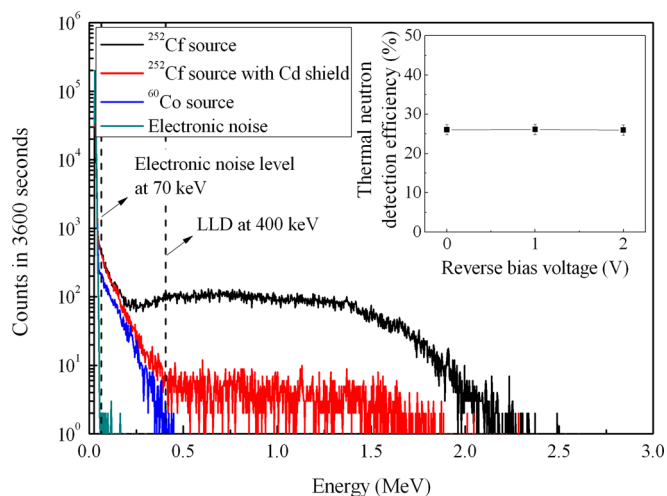


FIG. 4. Measured pulse height distribution for a $2.5 \times 2.5 \text{ mm}^2$ enriched boron (99.9%) filled honeycomb structured neutron detector under zero bias voltage. The counts were recorded for 3600 s and the LLD was set at 400 keV. The inset shows the plot for neutron detection efficiency as a function of reverse bias voltage.

block thermal neutrons and allow fast neutrons and gamma rays to pass (red curve). In order to measure the gamma sensitivity, the detector was exposed with a cobalt-60 (^{60}Co) source, which produces 10 mR/h dose at a distance of 4 cm (blue curve). Finally, the background signal resulted from the electronic noise was measured with the ^{252}Cf removed from the room (green curve). It is clearly observed that the electronic noise level is below 70 keV. This electronic noise level includes noise due to the leakage current and other noise from the electronic system. Although the electronic noise level is very low, the neutron detector also responds to gamma rays, which are registered below 400 keV. In order to avoid any contribution from gamma rays to the intrinsic neutron detection efficiency, the low level discriminator (LLD) was set at 400 keV. The Maxwellian averaged thermal neutron detection efficiency without bias is $26.1\% \pm 0.3\%$ and the gamma sensitivity is $\sim 10^{-5}$. Same thermal neutron detection efficiencies were measured under the reverse bias voltage of 1 and 2 V, which shows that the Si wall has been fully depleted by the continuous $\text{p}^+\text{-n}$ junction without bias.

In summary, J-V characteristics for planar $\text{p}^+\text{-n}$ diodes fabricated by depositing and diffusing boron at different diffusion temperatures (700, 800, and 900 °C) as a part of boron

filling process using LPCVD were studied. J-V characteristics show that diffusion at 800 and 900 °C results in reasonably good diode behavior and lower reverse leakage current compared to diffusion at 700 °C. A $2.5 \times 2.5 \text{ mm}^2$ ^{10}B filled honeycomb structured neutron detector with a continuous $\text{p}^+\text{-n}$ junction formed by using the initial portion of boron filling process shows the leakage current density of $\sim 2 \times 10^{-8} \text{ A/cm}^2$ at -1 V , which is comparable to that of a planar detector. Furthermore, thermal neutron detection efficiency of $\sim 26\%$ was achieved for a single layer detector and the efficiency is found to be independent of applied reverse bias voltage due to the fully depleted Si wall. These results are very promising for the emerging field of solid-state neutron detector applications.

The authors would like to thank the support and input of the support staff of the Rensselaer Polytechnic Institute MicroNano-Clean-Room (RPI MNCR) and Cornell NanoScale Science & Technology Facility (CNF). This work was supported by DOE—Nuclear Energy University Programs (NEUP), Award No. DE-AC07-05ID14517.

- ¹A. Rose, *Nucl. Instrum. Methods* **52**, 166 (1967).
- ²C. Petrillo, F. Sacchetti, O. Toker, and N. J. Rhodes, *Nucl. Instrum. Methods Phys. Res. A* **378**, 541 (1996).
- ³D. S. McGregor, M. D. Hammig, Y.-H. Yang, H. K. Gersch, and R. T. Klann, *Nucl. Instrum. Methods Phys. Res. A* **500**, 272 (2003).
- ⁴D. S. McGregora, R. T. Klann, H. K. Gersch, and Y.-H. Yang, *Nucl. Instrum. Methods Phys. Res. A* **466**, 126 (2001).
- ⁵R. J. Nikolic, A. M. Conway, C. E. Reinhardt, R. T. Graff, T. F. Wang, N. Deo, and C. L. Cheung, *Appl. Phys. Lett.* **93**, 133502 (2008).
- ⁶D. S. McGregor, W. J. McNeil, S. L. Bellinger, T. C. Unruh, and J. K. Shultis, *Nucl. Instrum. Methods Phys. Res. A* **608**, 125–131 (2009).
- ⁷N. LiCausi, J. Dingley, Y. Danon, J.-Q. Lu, and I. B. Bhat, *Proc. SPIE* **7079**, 707908 (2008).
- ⁸H. P. Yoon, Y. A. Yuwen, C. E. Kendrick, G. D. Barber, N. J. Podraza, J. M. Redwing, T. E. Mallouk, C. R. Wronski, and T. S. Mayer, *Appl. Phys. Lett.* **96**, 213503 (2010).
- ⁹K.-C. Huang, R. Dahal, J. J.-Q. Lu, Y. Danon, and I. B. Bhat, *J. Vac. Sci. Technol. B* **30**, 051204 (2012).
- ¹⁰F. Sarubbi, T. L. M. Scholtes, and L. K. Nanver, *J. Electron. Mater.* **39**, 162–173 (2010).
- ¹¹F. Laermer, A. Urban, and R. Bosch, in *13th International Conference on Solid-State Sensors, Actuators and Microsystems Stuttgart, Germany, 5–9 June 2005* (IEEE, New York, 2005), Vol. 2, pp. 1118–1121.
- ¹²R. Dahal, K.-C. Huang, J. Clinton, N. Licausi, J.-Q. Lu, Y. Danon, and I. B. Bhat, *Appl. Phys. Lett.* **100**, 243507 (2012).
- ¹³S. Agostinelli, J. Allison, K. Amako, J. Apostolakis, H. Araujo, P. Arce, M. Asai, D. Axen, S. Banerjee, and G. Barrand, *Nucl. Instrum. Methods Phys. Res. A* **506**, 250 (2003).